DESIGN OF COMPACT COUPLED MICROSTRIP LINE BAND PASS FILTER WITH IMPROVED STOPBAND CHARACTERISTICS

A. K. Tiwary[*] and N. Gupta

Department of Electronics and Communication Engineering, Birla Institute of Technology, Mesra, Ranchi 835215, India

Abstract—A compact symmetrical band-pass filter design using coupled microstrip line is presented in this paper. The microstrip line sections connected to the two input and output ports of the filter structure are printed over the Defected Ground Structure (DGS). The proposed symmetrical structure offers a simple and compact design and exhibits improved stop-band characteristics in comparison to the conventional coupled microstrip line filter structure. The prototype model of the proposed filter structure is developed and tested. The measured results are found to be in good agreement with the simulation results.

1. INTRODUCTION

Microwave band-pass filters play important roles in the microwave systems especially in the transmitting and receiving systems to identify and transmit the desired signals. As for the planar microwave band-pass filters, there are normally four different types: the combline filters, the interdigital filters, the parallel coupled filters and the hairpin-line filters. In modern RF/microwave communication systems, the size of the planar microwave filters is one of the major concerns, especially when these filters are applied in the monolithic microwave integrated circuits (MMIC). As for the miniaturization of the microwave filters, numerous methods were proposed in the past [1–7]. Among them, the use of high dielectric constant substrate, the slow-wave effect and the stepped-impedance resonator (SIR) structure are the most effective techniques to achieve compact size. In this paper, an attempt is made to design a compact coupled microstrip line filter with

improved performance characteristics by making use of symmetrical filter configuration printed on DGS. First, a prototype band-pass filter based on conventional asymmetrical parallel coupled microstrip line [8–11] configuration is designed. A simple design procedure for the coupled microstrip line band-pass filter can be found in [8]. The design is further modified to realize a compact symmetrical parallel coupled band-pass configuration [12] by printing the lower diagonal portion of the coupled lines in the upper right half portion so as to form a symmetrical compact bandpass filter structure occupying practically half the area than the conventional asymmetrical parallel microstrip configuration. Finally the characteristics of the compact structure are further improved by realizing the I/O sections of the microstrip feed lines on DGS.

2. FILTER DESIGN

The parallel-coupled microstrip transmission lines can be used to construct many types of filters. The general conventional BPF structure of the parallel-coupled-line filter is based on the half-wavelength resonators. The proposed filter structure is constructed on the FR4, PCB board with dielectric constant $\varepsilon_r = 4.4$, loss tangent $\tan \delta = 0.016$ and substrate thickness $h = 1.6\,\text{mm}$. The Method of Moments based IE3D version 9.35 simulation software from Zeland USA is used for the purpose of simulation. The filter design can be maximally flat (Butterworth) or with ripple value (Chebyshev). In the present work a Chebyshev design is used. The Fractional Bandwidth (FBW) is set to FBW = 15% and the specified pass-band ripple to $0.1\,\text{dB}$ with the central frequency $f_0 = 2.4\,\text{GHz}$. Considering these specifications, the element values of the prototype Chebyshev low-pass filter with pass-band ripple of $0.1\,\text{dB}$, are selected as $g_0 = g_6 = 1.0$, $g_1 = g_5 = 1.1468$, $g_2 = g_4 = 1.3712$, $g_3 = 1.9750$.

$$\frac{J_{01}}{Y_0} = \sqrt{\frac{\Pi \times \Delta}{2 \times g_0 \times g_1}} \tag{1}$$

$$\left.\frac{J_{j,j+1}}{Y_0}\right|_{j=1 \ to \ n-1} = \frac{\Pi \times \Delta}{2 \times \sqrt{g_j \, g_{j+1}}} \tag{2}$$

$$\frac{J_{n,n+1}}{Y_0} = \sqrt{\frac{\Pi \times \Delta}{2 \times g_n \times g_{n+1}}} \tag{3}$$

where g_0, g_1, ..., g_{n+1} are the elements value of the low-pass prototype filter with a normalized cutoff $\Omega_c = 1$. The $J_{j,\,j+1}$ are admittance inverter parameters and Y_0 is the characteristic admittance

Table 1. Design parameters for parallel-coupled strip-line resonator filter.

j	$J_{j,j+1}/Y_0$	$(Z_{oe})_{j,j+1}$	$(Z_{oo})_{j,j+1}$	$W_{j,\,j+1}$ (mm)	$s_{j,\,j+1}$ (mm)	$d_{j,\,j+1}$ (mm)
0	0.45316	82.9257	37.6097	0.48	0.412	0.264
1	0.1878	61.1534	42.3734	0.64	0.5	0.264
2	0.1431	58.1789	43.8689	0.704	0.58	0.264

of the terminating lines. The even-mode and odd-mode impedance of the strips are

$$(Z_{oe})_{j\,,\,j+1}\Big|_{j=0\,to\,n} = \frac{1}{Y_0}\left[1 + \frac{J_{j,j+1}}{Y_0} + \left(\frac{J_{j,j+1}}{Y_0}\right)^2\right] \qquad (4)$$

$$(Z_{oo})_{j\,,\,j+1}\Big|_{j=0\,to\,n} = \frac{1}{Y_0}\left[1 - \frac{J_{j,j+1}}{Y_0} + \left(\frac{J_{j,j+1}}{Y_0}\right)^2\right] \qquad (5)$$

The $J_{j,\,j+1}/Y_0$, $(Z_{oe})_{j,\,j+1}$, and $(Z_{oo})_{j,\,j+1}$ values are calculated from the Equations (1) to (5). The dimensions of the strip width $W_{j,\,j+1}$, and the gaps are obtained from the given graphs [13].

The basic length l is a quarter-wavelength at frequency ω_0 in the medium of propagation, while the actual length is shorted by the amount $d_{j,\,j+1}$. Cohn [13] has found that a constant correction of $d_{j,\,j+1} = 0.165b$ (where b is the ground-plane spacing). The dimensions $d_{j,\,j+1}$ are resonator length corrections to account for the fringing capacitance from the end of each strip. The top view of the conventional parallel-coupled BPF is shown in Figure 1(a). The ground plane is complete metallic structure. In the Simulation the ground plane is considered to be finite with a total substrate area of $136\,\text{mm} \times 12.5\,\text{mm} = 1700\,\text{mm}^2$.

To reduce the area occupied by the conventional filter structure the compact parallel coupled Band-pass filter is realized as shown in Figure 1(b). The compact structure occupies overall area of $136\,\text{mm} \times 6.60\,\text{mm} = 897.6\,\text{mm}^2$.

The simulated results for the S-parameter characteristics of the conventional BPF and the compact BPF are shown in Figure 2. A comparison of the two results shows that the conventional and the compact BPF exhibit similar characteristics. Reduction in area (%) can be calculated as $((1700 - 897.6)/1700) * 100 \cong 47\,\%$. However, in compact BPF the overall size reduction of approx. 47 percent is achieved in comparison to the conventional BPF.
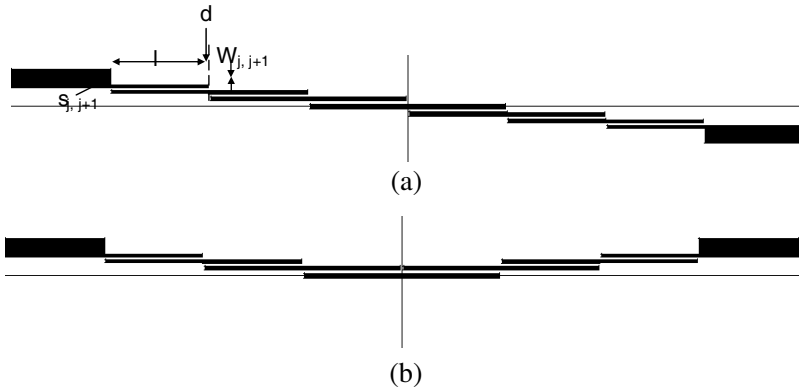
Figure 1. (a) The conventional parallel-coupled BPF (top view). (b) The compact parallel-coupled BPF (top view).
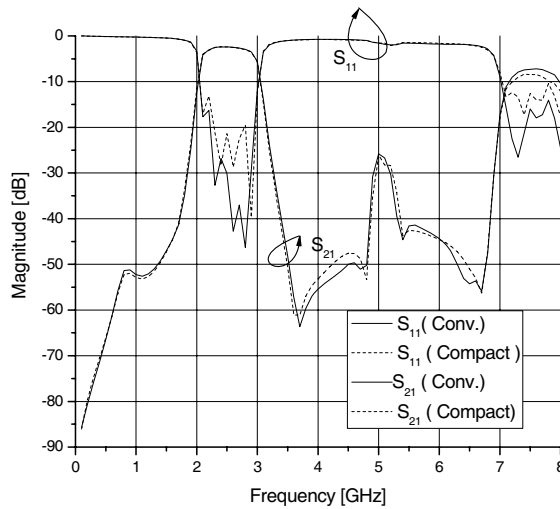

Figure 2. Simulated S-parameter characteristics of conventional and compact BPF.

The S-parameter characteristics also show a limited stop-band characteristics ranging from approximately 3 to 7 GHz due to the occurrence of the higher harmonics. In order to widen the stop band characteristics the use of Defected Ground Structure (DGS) is proposed. The I/P and O/P microstrip line feeding structure is printed over DGS sections both at the input and output ports as
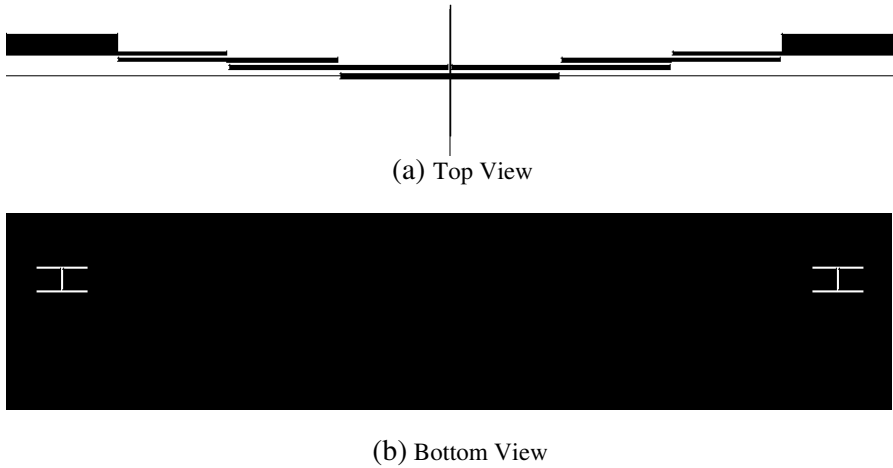
(a) Top View

(b) Bottom View

Figure 3. The proposed compact parallel coupled line BPF on DGS.

shown in Figure 3. The DGS configuration proposed in this work is a dumb-bell shaped structure which is capable of exhibiting the desired stop band characteristics without disturbing the pass band characteristics. In fact, a DGS in the ground plane disturbs the shield current distribution in the ground plane and this disturbance in turn changes in characteristics of the transmission line in terms of line capacitance and inductance. The self resonant characteristic of the proposed DGS helps the BPF to exhibit an attenuation pole in the upper stop-band region. By properly selecting the geometrical parameters of the proposed DGS shape, the attenuation pole can be forced to occur at the desired location in the frequency band of interest and thus the stop band can easily be widened in comparison with the conventional coupled line filters.

Figure 3 shows the proposed coupled-line band-pass filter with two DGS sections, which is located on the metallic ground plane below the I/O transmission lines.

In order to derive an equivalent circuit for the proposed parallel coupled-line BPF, an equivalent circuit and extraction method approach of the circuit parameters for a DGS [2, 3], is employed. The circuit representation of the five-pole coupled-line BPF with equivalent circuits of the DGS, represented by a parallel LC circuit is shown in Figure 4. The series susceptance for a parallel LC resonator, shown in Figure 5(a), can be converted to a parallel resonator with a J-inverter as shown in Figure 5(b).
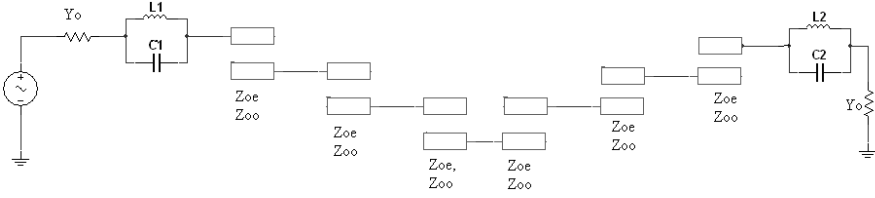
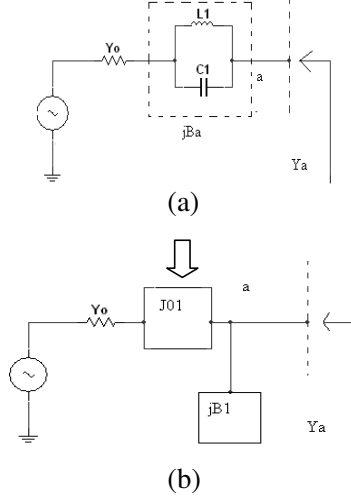**Figure 4.** Circuit representation of the proposed BPF.

(a)

(b)

Figure 5. Converting LC resonator circuit into a J-inverter and a parallel resonator.

The J-inverter formula and resonator susceptance are given by

$$J_{01} = \sqrt{\frac{B_a^2}{1 + \left(\frac{B_a}{Y_0}\right)^2}} \tag{6}$$

$$B_1 = \frac{B_a}{1 + \left(\frac{B_a}{Y_0}\right)^2} \tag{7}$$

$$B_a = \omega_{C1} \cdot C_1 \left(\frac{\omega}{\omega_{C1}} - \frac{\omega_{C1}}{\omega}\right) \tag{8}$$

where, B_a is susceptance of the DGS section, B_1 is the susceptance of the equivalent resonator for the DGS section, ω_{C1} is the angular resonant frequency of the parallel LC resonator and C_1 denotes the

extracted capacitances. At this resonant frequency of the DGS circuit, the J-inverter value becomes zero indicating that there is no coupling at this frequency such as dc. Thus, the proposed band-pass filter structure can provide an attenuation pole at the resonant frequency of the DGS circuit.

3. PARAMETRIC STUDY

3.1. Influence of the Lattice Dimension

In order to examine the influence of the lattice dimension, a microstrip line with $50\,\Omega$ characteristics impedance printed over the dumbbell DGS section is considered. The microstrip line with etched lattice shape of the proposed DGS section located on the metallic ground plane is shown in Figures 6(a) and (b). The structure is constructed on the FR4, PCB board with dielectric constant $\varepsilon_r = 4.4$, loss tangent $\tan\delta = 0.016$ and substrate thickness $h = 1.6\,\text{mm}$ for all simulations since the proposed filter is constructed on the same substrate. The DGS unit section can provide cutoff frequency and attenuation pole at some frequency without any need for periodic array of DGS. The etched gap, which is related to the gap capacitance, is kept constant to $0.5\,\text{mm}$ for all the cases to facilitate the fabrication tolerances and the etched area is varied (along x and y axis). The S-parameter characteristics of the structure are shown in Figure 7. The results obtained for various lattice dimensions are summarized in Table 2. As the etched area of the unit lattice is increased, the effective series inductance increases, and increase in the series inductance gives rise to a lower cutoff frequency and a shift in the corresponding location of the attenuation poles. These attenuation poles can be explained by parallel capacitance with the series inductance. This capacitance depends on the etched gap below the conductor line, which is denoted
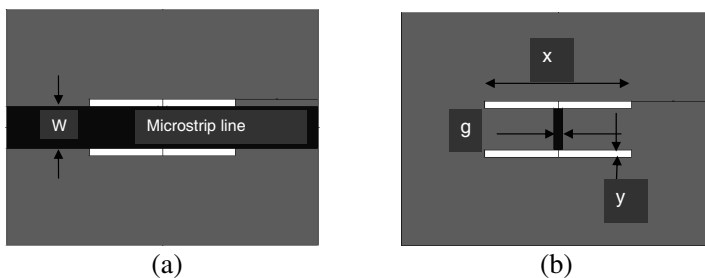

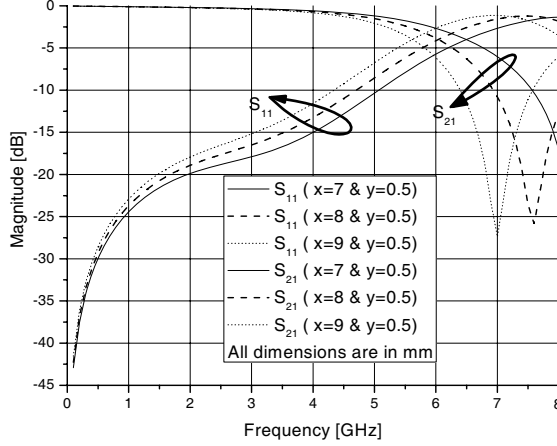Figure 6. Top view & bottom view of Microstrip line with DGS.

Figure 7. Effect of Lattice dimension on S_{11} and S_{21}.

by g in Figure 6(b). However, the attenuation pole location, which corresponds to the resonance frequency of the parallel LC circuit, also shifts toward lower frequency range because of the fact that as the series inductance increases, the resonance frequency of the equivalent parallel LC circuit decreases.

3.2. Modeling and Parameter Extraction

In the previous section, it is shown that the parallel LC circuit represents the equivalent circuit of the proposed DGS section. From a practical point of view, the DGS section can serve as replacements for a parallel LC resonator circuit. To apply the proposed DGS section to a practical circuit design, it is essential to extract the equivalent circuit parameters. The equivalent circuit of the proposed DGS is shown in Figure 8 and the Butterworth-type one-pole prototype low-pass filter circuit is shown in Figure 9.

The reactance value of the proposed DGS unit can be expressed as follows:

$$X_{LC} = \frac{1}{\omega_0 C} \left(\frac{\omega_0}{\omega} - \frac{\omega}{\omega_0} \right) \tag{9}$$

where, ω_0 is the resonance angular frequency of the parallel LC resonator, which is corresponding to attenuation pole location in Figure 7. The series inductance of the Butterworth low-pass filter can be derived as follows:

$$X_L = \omega' \cdot Z_0 g_1 \tag{10}$$

Table 2. Attenuation pole locations for different lattice dimensions.

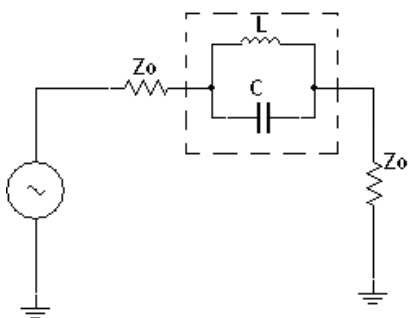| No. of Set	x (mm)	y (mm)	Cut off frequency (GHz)	Attenuation Pole location (GHz)
	9	0.5	5.3	7
I	8	0.5	5.7	7.5
	7	0.5	6.1	8.2
	7	1	5.3	7.5
II	6.5	1	5.7	7.8
	6	1	6.2	8.1
	5	1	6.8	9
III	4.1	3.1	4.4	7.5
IV	3.5	3.5	4.5	7.5

Figure 8. Equivalent circuit of the proposed DGS section.
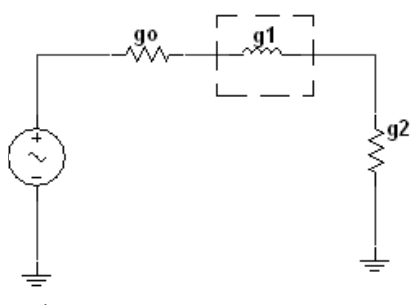
Figure 9. Butterworth-type one-pole prototype low-pass filter circuit.

where ω' denotes the normalized angular frequency, Z_0 denotes the scaled impedance level of the in/out terminated ports, and g_1 is given by the prototype value of the Butterworth-type low pass filter. In order equate the two characteristics, the reactance of the proposed DGS unit section, shown in Figure 8, is matched with the reactance of the prototype low-pass filter, shown in Figure 9, at the desired frequency.

Table 3. Equivalent-circuit parameters extraction.

Equivalent circuit parameters	DGS dimensions (mm) gap distance $g = 0.5$ mm			
	$x = 8$ $y = 0.5$	$x = 7$ $y = 1$	$x = 4.1$ $y = 3.1$	$x = 3.5$ $y = 3.5$
Inductance (nH)	1.148	1.437	2.266	2.207
Capacitance (pF)	0.392	0.313	0.199	0.204
Cutoff Frequency GHz)	5.73992	5.3788	4.49746	4.55327
Attenuation pole Location (GHz)	7.5	7.5	7.5	7.5

The equality at the cutoff frequency of the low-pass filter is given as:

$$X_{LC}|_{\omega=\omega_C} = X_L|_{\omega'=1} \tag{11}$$

From the above equality, the series capacitance C of the equivalent circuit, shown in Figure 8, is obtained as follows:

$$C = \frac{\omega_C}{Z_0 g_1} \cdot \frac{1}{\omega_0^2 - \omega_C^2} \tag{12}$$

Once the capacitance value of the equivalent circuit is extracted, the series equivalent inductance for the given DGS section can be calculated as follows:

$$L = \frac{1}{4\Pi^2 f_0^2 \cdot C} \tag{13}$$

where, f_0 is the frequency of the attenuation pole location and C is the extracted series capacitance value.

Next, only the set of x and y parameters for which the attenuation pole occurs precisely at 7.5 GHz are selected from Table 2 and the equivalent circuit parameters L and C are extracted only for these cases as stated above. The results obtained are tabulated in Table 3.

The S-parameter characteristics for various combinations of x and y is shown in Figure 10. By selecting $x = 8$ mm and $y = 0.5$ mm, a combination of higher capacitance and lower value of inductance is achieved. This data is considered for the proposed work. As evident, the stop band characteristics are widened from 3 GHz to 8 GHz.

A comparison of the S-parameter characteristics (both simulated and experimental) obtained for the proposed filter with and without DGS section is shown in Figure 11.
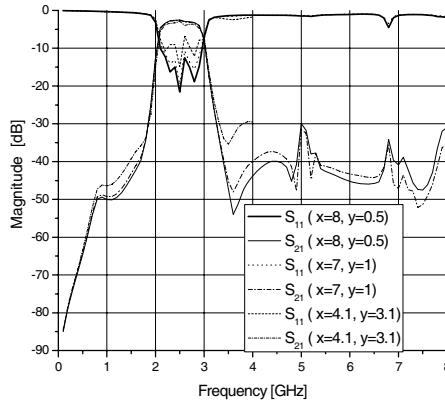
Figure 10. S-parameter characteristics for various value of x and y (DGS).
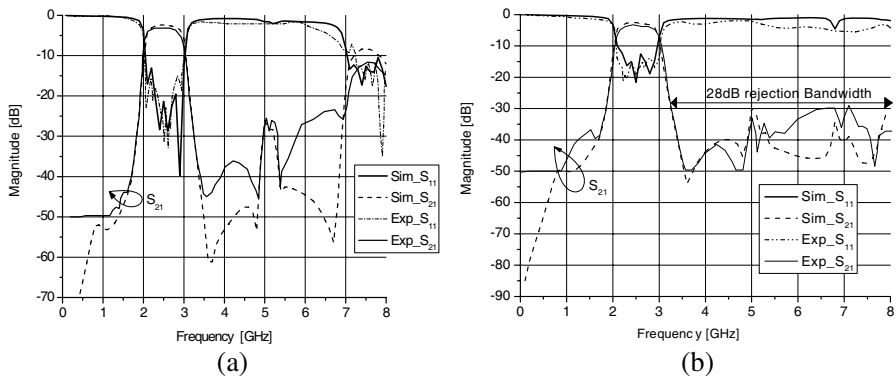

Figure 11. (a) Simulated and experimental S-parameter characteristics of compact BPF. (b) Simulated and experimental S-parameter characteristics of proposed BPF.

The prototype models developed on the inexpensive FR4 substrate with a dielectric constant of 4.4 and thickness of 1.6 mm are shown in Figures 12(a), (b), and 12(c), (d).

4. FABRICATION AND MEASUREMENTS

The proposed BPF with DGS section is realized using microstrip technology. The prototype model is developed and then the characteristics are measured by using Vector Network Analyzer. The comparison between the simulated and the experimental results is
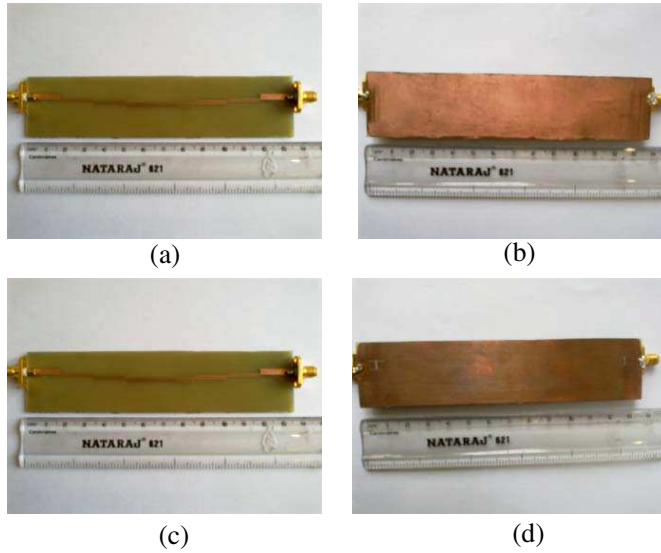
Figure 12. (a) and (b): top and bottom views, respectively, of compact BPF (fabricated). (c) and (d): top and bottom views, respectively, of proposed BPF (fabricated).

shown in Figure 11. A good agreement between the two is evident. The simulated and measured results both confirm that the proposed BPF configuration posses better performance in terms of high out-of-band rejection level. The top and bottom view of fabricated BPF with and without DGS is shown in Figures 12(a), (b) and 12(c), (d).

5. CONCLUSION

A compact symmetrical parallel coupled BPF design etched on the DGS lattice section is realized. The proposed design not only occupies approximately half of the area required by the conventional BPF structure but also offers improved stop band characteristics. The proposed structure finds application in WLAN devices.

REFERENCES

1. Chang, C. Y. and T. Itoh, "Modified parallel couple filter structures that improve the upper stopband rejection and response symmetry," *IEEE Trans. Microwave Theory Tech.*, Vol. 39, 310–314, 1991.

2. Ester, B. and K. A. Merze, "Parallel couple line filters for inverted microstrip and suspended substrates MICs," *11th European Microwave Conference Digest*, 164–167, 1981.

3. Park, J. S., J. S. Yun, and D. Ahn, "A design of the novel coupled-line bandpass filter using defected ground structure with wide stopband performance," *IEEE Trans. Microwave Theory Tech.*, Vol. 50, 2037–2043, 2002.

4. Mollah, M. N., N. C. Karmakar, and J. S. Fu, "Uniform circular photonic bandgap structures (PBGSs) for harmonic suppression of a bandpass filter," *International Journal of Electronics & Communication*, Vol. 62, 717–724, 2008.

5. Kuo, J. T. and H. P. Lin, "Dual-band bandpass filter with improved performance in extended upper rejection band," *IEEE Trans. Microwave Theory Tech.*, Vol. 57, 824–829, 2009.

6. Wu, C. H., C. H. Wang, and C. H. Chen, "Stopband-extended balanced bandpass filter using coupled stepped-impedance resonators," *IEEE Microwave Wireless Compon. Lett.*, Vol. 17, 507–509, 2007.

7. Ye, C.-S., Y.-K. Su, M.-H. Weng, C.-Y. Hung, and R.-Y. Yang, "Design of the compact parallel-coupled lines wideband bandpass filters using image parameter method," *Progress In Electromagnetics Research*, Vol. 100, 153–173, 2010.

8. Hong, J. S. and M. J. Lancaster, *Microstrip Filters for RF/microwave Applications*, Wiley, New York, 2001.

9. Mohra, A. S., "Coupled microstrip line bandpass filter with harmonic suppression using right-angle triangle grooves," *Microwave Opt. Technol. Lett.*, Vol. 51, 2313–2318, 2009.

10. Garcia, J. G., F. Martin, F. Falcone, J. Bonache, I. Gil, T. Lopetegi, M. A. G. Laso, M. Sorolla, and R. Marques, "Spurious passband suppression in microstrip coupled line band pass filters by means of split ring resonators," *IEEE Microwave Wireless Compon. Lett.*, Vol. 14, 416–418, 2004.

11. Chin, K. S., Y. C. Chiou, and J. T. Kuo, "New synthesis of parallel-coupled line bandpass filters with Chebyshev responses," *IEEE Trans. Microwave Theory Tech.*, Vol. 56, 1516-01523, 2008.

12. Kung, C. Y., Y. C. Chen, C. F. Yang, and C. Y. Huang, "Triple-band parallel coupled microstrip bandpass filter with dual coupled length," *Microwave Opt. Technol Lett.*, Vol. 51, 995–997, 2009.

13. Mattaei, G., L. Young, and E. M. T. Jones, *Microwave Filters, Impedance-matching Networks, and Coupling Structures*, Artech House, Norwood, MA, 1980.